Archives of Oral Biology 178 (2025) 106368

Contents lists available at ScienceDirect

Archives of Oral Biology

journal homepage: www.elsevier.com/locate/archoralbio

Transplanted mesenchymal stem cells isolated from the bone marrow ameliorate the histological alterations in the parotid glands of hypothyroid male rats

Hanan El-Hemedy [a,1], Mohamed Badawy [a,2], Mary Moheb [b,3], Maha El Shahawy [b,c,*,4]

[a] Department of Oral Biology, Faculty of Dentistry, Assiut University, Assiut 71515, Egypt
[b] Department of Oral Biology, Faculty of Dentistry, Minia University, Misr Aswan Road, Minia 61511, Egypt
[c] Department of Oral Biology, Faculty of Dentistry, Kafrelsheikh University, Elgiesh street, Kafrelsheikh 33516, Egypt

ARTICLE INFO

Keywords:
Mesenchymal stem cells
Parotid Gland
Hypothyroid rats
histology
histomorphometry

ABSTRACT

Objective: To elucidate the possible outcome of mesenchymal stem cells extracted from the bone marrow (BM-MSCs) on the altered histological structure of the parotid gland of male rats with induced hypothyroidism.
Design: 24 adult male Wistar rats were used. The rats were divided into 3 groups, each containing 8 animals. The control group contained the sham-operated animals. The hypothyroid rat group (HT group) contained animals receiving carbimazole at a dose of 20 mg/kg per day up to 6 weeks to induce hypothyroidism. The third group contained rats with induced hypothyroidism and were administered BM-MSCs via the tail vein (HT-MSC) group. BM-MSCs were extracted from 3-week-old rats and were immunophenotyped prior to injection to the HT-MSC group. The parotid glands were dissected 6 weeks post injection and processed to assess PKH67-labelled cells, histomorphometry and staining with Haematoxylin and Eosin (H and E).
Results: Rats with induced hypothyroidism depicted a significant decrease in the thyroid hormones' serum levels. Extracted BM-MSCs were CD105 + , CD90 + and $CD45^-$. The parotid gland of HT group depicted an abnormal structure of the acini, intercalated, striated and excretory ducts including nuclear alterations, vacuolization and indistinct boundaries compared to their controls. In addition, the area and perimeter of the acini were diminished. The HT-MSCs group depicted green $PKH67^+$-labelled MSCs, restoration of the normal acinar and ductal configuration, and regular area and perimeter of the acini.
Conclusion: Transplanted BM-MSCs resumed the normal parotid gland acinar, intercalated, striated and excretory duct structure in the hypothyroid male rats, suggesting restored tissue function.

1. Introduction

Salivary glands are essential for secreting saliva that is pivotal for speaking, eating, swallowing, and digesting food (Ghannam & Singh, 2022). The parotid gland is the largest paired salivary gland and its parenchymal components are divided into lobes and lobules by the connective tissue septa. The parenchymal portion includes the duct system and secretory serous acini. The intralobular ducts include the intercalated and striated, the latter evacuates into a larger interlobular excretory duct (Nanci, 2018).

The thyroid gland secretes thyroid hormones that are virtually critical in the growth and maintenance of all the body organs and tissues. The thyroid hormones are essential for normal cell growth, proper cell differentiation, development (Hofstee et al., 2019), regulation of the

Abbreviations: BM-MSCs, mesenchymal stem cells extracted from the bone marrow; H and E, Hematoxylin and Eosin; HT group, hypothyroid rat group; HT-MSC group, hypothyroid rat group received; BM-MSC, injection.

* Corresponding author at: Department of Oral Biology, Faculty of Dentistry, Minia University, Misr Aswan Road, Minia 61511, Egypt.
E-mail addresses: Hanan.elhamady@dent.aun.edu.eg (H. El-Hemedy), mbadawy@aun.edu.eg (M. Badawy), mery.moheb@mu.edu.eg (M. Moheb), maha.elshahawy@minia.edu.eg (M. El Shahawy).
[1] ORCID: 0009–0000-4680–4491
[2] ORCID: 0000–0003-0357–6577
[3] ORCID: 0000–0001-8053–4851
[4] ORCID: 0000–0001-7122–1191

https://doi.org/10.1016/j.archoralbio.2025.106368
Received 23 April 2025; Received in revised form 1 August 2025; Accepted 2 August 2025
Available online 6 August 2025

metabolic rate and protein synthesis (Al-Suhaimi & Khan, 2022; Schneider et al., 2023). One of the most common thyroid disorders is hypothyroidism which is caused by a decrease in the production of thyroid hormones resulting from damage, removal, or functional inhibition of the thyroid gland (Bordbar et al., 2024). In addition, it can be a consequence of complications from the treatment of hyperthyroidism by carbimazole (Reyad et al., 2021). Oral symptoms of hypothyroidism may include tongue swelling, increased vulnerability to dental cavities, enlarged salivary glands (Mostafa, 2022), and hyposalivation (Hashem & Saad, 2019). Abnormal parotid and submandibular gland architecture and function were observed in the hypothyroid rats (Hayat et al., 2010, 2016; Ayuob, 2016; Elazeem et al., 2016; Nasr El-Din & Abdel Fattah, 2020; Alhahawachee et al., 2022; Pimentel et al., 2022; Uzun et al., 2022). Therefore, thyroid hormones are essential for preserving the histology and function of the salivary glands in a normal manner (Alhahawachee et al., 2022).

Impaired salivary gland function leads to a lower quality of the patient's life due to halitosis, persistent burning sensation, altered taste perception and difficulties in swallowing, speaking, and eating (Ito et al., 2023). The effectiveness of various treatment methods for hyposalivation is debatable (Quimby et al., 2020). Artificial lubricants provide only momentary relief (Nam et al., 2023); therefore, alternative therapeutic methods are needed, and regenerative medicine is an attractive approach to regenerate salivary tissue structure and function.

Stem cells attracted the interest of many scientists in recent years (Muallah et al., 2023). Mesenchymal stem cells (MSCs) were extracted from adipose tissue, hair follicles, cornea, dental pulp, peripheral blood, and bone marrow (Jammes et al., 2025). MSCs are capable of homing to the inflammatory sites during tissue injury and can characterize into multiple cell identities such as fat cells, muscle, cartilage, connective tissue, and bone. In addition, they increase angiogenesis and secrete various bioactive molecules that promote the healing of the injured cells (Han et al., 2022; Yang et al., 2023). MSCs extracted from the bone marrow (BM-MSCs) are among the first identified MSCs and are commonly used in clinical trials. Transplanted BM-MSCs restored the normal structure of different organs of various conditions including the tongue of diabetic rats (Radwan et al., 2024) and of the hypothyroid animals (Mahmoud et al., 2024), parotid glands of diabetic animal model (Denewar & Amin, 2020), submandibular glands of rats with ovariectomy (El-Badawy et al., 2024) and of hypothyroid rats (El dahrawy et al., 2021), submandibular gland degenerative changes induced by cisplatin (Zakaria et al., 2025), and recently in preserving the ultrastructure of the organ of Corti in animal model with induced loss of hearing (Abdelwahed et al., 2025).

Several types of stem cell have been employed in the treatment of degenerative changes in the parotid gland of various conditions including gingival-derived mesenchymal stem cells in irradiated parotid glands (Zayed et al., 2024), umbilical cord blood mesenchymal stem cells in glands of ovariectomized animals (El-naseery et al., 2018), adipose tissue-derived stem cells in irradiated parotid (Wang et al., 2017), dental pulp stem cells in diabetic rat glands (Al-Serwi et al., 2021).

Although the impact of transplanted MSCs of adipose tissue, umbilical cord, dental pulp and gingival origins on the altered architecture of the parotid gland of rats with induced hypothyroidism has been elucidated (Wang et al., 2017; El-naseery et al., 2018; Al-Serwi et al., 2021; Zayed et al., 2024), there is deficiency in studies evaluating the potential therapeutic use of BM-MSCs in the abnormal parotid gland structure of hypothyroid rats. In the present work, we hypothesized that transplanted BM-MSCs impact the architectural alterations of the parotid gland of hypothyroid male rats. We, therefore, evaluated the possible outcome of transplanted BM-MSCs on parotid gland histological changes in hypothyroid male rats.

2. Materials and methods

The Faculty of Dentistry's Research Ethics Committee, at Minia University approved all the animal experimental procedures (Code: RHDIRB2017122001, Decision No. 590). The experimental work complies with the national and ARRIVE guidelines as well as Guide to the Care and Use of Laboratory Animals by National Research Council (Council, 2011; Percie du Sert et al., 2020).

2.1. Isolation and characterization of the BM-MSCs

Isolation of the MSCs and their immunophenotyping were done as described in the previous work (El-Badawy et al., 2024; Mahmoud et al., 2024), followed by their injection to the HT-MSC group. The MSCs were extracted from the hind limbs of two male rats of three-week-old. After disinfection and incision of the skin, the excision of the hind limb was performed with sterilized scissor and all the muscles and ligaments were carefully dissected. The heads of the hind limb bone was removed. Three ml of Low-Glucose DMEM (Invitrogen Life Technologies, Gibco, Carlsbad, CA, USA), Amphotericin B (25 g), 1 % penicillin G sodium (10.000 UI), streptomycin (10 mg), 10 % FBS exosome-free (Gibco, Thermo Scientific, Germany) were utilized to completely flush the medulla. A sterile syringe supplemented with needle (18-gauge), was utilized to suck and dispense the medium and the cells to get single cell suspension. This was followed by 10 min centrifugation at 2000 rpm, at 4 °C. The obtained pellet was resuspended in culture media after discarding the floating aspirate (El-Badawy et al., 2024; Mahmoud et al., 2024).

The T-25 ml culture flask containing 100,000 cells in the bone marrow suspensions was incubated in 5 % CO_2, at 37 °C in the air. A series of PBS washes and subsequent media changes were performed to get rid of the non-adherent cells, after two days (Thermo Fisher Scientific Inc., Waltham, MA, USA). Thereafter, the cells were incubated at 37°C, with twice media changes per week. After 14 days, the cells were harvested utilizing (0.01 % EDTA+ 0.25 % trypsin) after 70 % cell confluence and were plated at a cell density of 1×10^6 per flask. A hemocytometer was utilized for determination of the cell count. The fourth passage's cells were utilized for the subsequent assessment (El-Badawy et al., 2024; Mahmoud et al., 2024).

The stem cells were identified by their spindle shape and adherence. In addition, multiparametric characterization utilizing flowcytometry was performed using the following antibodies: anti CD45-PC5, anti CD105-FITC, and anti CD90-FITC (Thermo Fisher Scientific, USA), to confirm the MSC identity. The cell count was adjusted to 10^6/ml. After suspending the cells in PBS, centrifugation was performed at 800 xg for 10 min. The pellet was washed in PBS twice, after discarding the aspirate. 5 μL of each antibody was utilized and two antibodies were added per tube (CD45/CD90, CD45/CD105), to reduce the autofluorescence. After 45 min of incubation at 4°C and washing the cells, the binding buffer was added. The flow cytometric results were analyzed utilizing *Navios software* (Beckman Coulter) (Heidari et al., 2021; Fathi & Farahzadi, 2022; El-Badawy et al., 2024).

2.2. The BM-MSC labelling by PKH67

To trace the isolated BM-MSCs, the *PKH67 Green Fluorescent Cell Linker Mini Kit* (MINI67–1KT, Sigma Aldrich, Saint Louis, USA) was utilized in labelling the MSCs. A staining mix was prepared of 1:1 of DMEM serum-free (Gibco, ThermoFisher, USA) and diluted dye solution, for each 1×10^6 cell culture. Then, the cells were incubated in 5 % CO_2 at 37°C for an hour, followed by removal of the staining mix to stop the staining process. Thereafter, the cells were incubated in a growth medium. After injection of the labelled BM-MSCs to the rats of the HT-MSC group, the dissected and processed parotid salivary glands were sectioned into 5-um thick sections. Under fluorescence microscope, the presence of the PKH67-labeled cells was assessed in these unstained 5-um sections (Labomed, Los-Anglos, USA) (El-Badawy et al., 2024; Mahmoud et al., 2024).

2.3. Experimental animals' grouping and hypothyroidism induction

24 healthy male adult Wister rats weighing 200– 250 g were kept at the animal facility at Assiut University, in controlled conditions of temperature (25 ± 1°C), humidity (30–35 %), and adequate ventilation. The rats were supplied with standard laboratory diet, food, and water *ad libitum* (El-Badawy et al., 2024).

Carbimazole was utilized for hypothyroidism induction. The medicine was provided in soluble tablet form (Chemical Industries Development, Giza, and A.R.E.), containing 5 mg of methimazole. To induce hypothyroidism, the animals were given 20 mg/kg of body weight per day of the drug after being dissolved in 12 ml of distilled water (Ajayi et al., 2018), by intragastric tube for 6 weeks (Mahmoud et al., 2024).

After one week of acclimatization, the animals were randomly distributed into 3 groups, with 8 animals for each. The control group contained animals administered 3 ml of distilled water orally by intragastric tube for six weeks to imitate the stress of the given drug. Thereafter, an IV injection at the lateral tail vein of 1 ml of cell-free media was performed. The hypothyroid rat group (HT group) contained hypothyroid rats receiving carbimazole for 6 weeks and thereafter received 1 ml of cell-free media. HT-MSC group included hypothyroid animals administered 1 ml of the culture media containing 1×10^6 of BM-MSCs (Mohsen et al., 2019). The animals were euthanized 6 weeks after the stem cells injection (Mahmoud et al., 2024).

To confirm hypothyroidism induction, the thyroid hormone levels were evaluated. Serum thyroxine and triiodothyronine were assessed six weeks after administration of carbimazole (Mahmoud et al., 2024). The blood specimens were stored for an hour at room temperature and centrifuged for 15 min at 3000 rpm. The extracted serum was kept at −20°C to be utilized for ELISA kit; Rat Thyroxine and Rat Triiodothyronine (Mybiosource, California, United States) (Ramadan Samaha, 2016).

2.4. Euthanasia, sample preparation and H and E staining

For euthanasia, the rats administered pentobarbital sodium (Nembutal, Akron, Illinois, USA) at a dose (120 mg/ kg) (Abdel Fattah & Omar, 2023). The heads were cervically dislocated, and the paired parotid glands were dissected. The glands were washed in PBS and preserved for 48 h in neutral buffered formalin (10 %) (El-Badawy et al., 2024).

The samples were rinsed in cold PBS followed by dehydration in ethanol, clearing in xylene and infiltration by paraffin as described previously (El-Badawy et al., 2024). The wax blocks were cut to 6 μm-thick sections and stretched over glass slides (StarFrost, Knittelglass, Germany). To assess the Parotid gland histology, the tissue sections were prepared for staining with H and E. First, parotid gland tissues were deparaffinized in 3 baths of xylene (5 min each), followed by rehydration in ethanol 99.5 %, 95 % and 70 % (3 baths each, 5 min each bath). Then, the sections were washed in distilled water and stained with H and E. At the end, the parotid gland sections were rinsed in tap water, dehydrated, xylene immersed, mounted, cover slipped (DPX EXTRA PURE, Alpha Chemika, India) and assessed under light microscope (DM LB100T, LEICA) (Cardiff et al., 2014; El-Badawy et al., 2024).

2.5. Acinar area and perimeter histomorphometry

The area and perimeter of the acini in the 3 studied groups were assessed utilizing Image J 22 Software (NIH, USA, version 1.48 v). For each group (n = 8), five non-overlapping fields were utilized for each sample at 200x magnification (Kurup et al., 2015).

2.6. Statistics

Statistical analysis of the serum thyroid hormones parameters in control and hypothyroid rats and the area and the perimeter of the acini of the 3 rat groups were performed utilizing non-parametric tests. Mann Whitney test was utilized to analyze the levels of thyroid hormones. The Kruskal Wallis test and thereafter the Post-hoc test (Dunn's for multiple comparison test) were utilized to analyse the acinar perimeter and area. The $p \leq 0.05$ was utilized as cut off value of significance. For statistical analysis, IBM SPSS software version 20.0 was utilized (Armonk, New York, IBM Corp.).

3. Results

3.1. Reduced levels of thyroid hormones in rats with induced hypothyroidism

The serum levels of thyroxine and triiodothyronine were analysed, and the data revealed that the hypothyroid rats had significantly lower serum hormones levels than their controls (5.93 ± 0.47, 91.53 ± 5.14, $p < 0.001$) (Figs. 2A, 2B), (Table 1).

3.2. Characterization and detection of the isolated MSCs

Multiparametric analysis revealed that most of the isolated cells were immuno-positive for CD105 and CD90 and co-expressed CD45 (Fig. 1A), depicting pure extraction of MSCs from the bone marrow. Parotid gland unstained tissues of the HT and control groups revealed negative staining with PKH67 (Figs. 1B, 1C); by contrast, the unstained parotid gland tissue sections from the HT-MSC group depicted PKH67 labelled BM-MSCs with green fluorescence (Fig. 1D).

3.3. Histological alterations of the parotid gland tissues of the hypothyroid rats and restoration of the normal gland histology in the HT-MSC treated rats

To assess whether BM-MSC transplantation could improve the abnormal histology of the parotid gland in the hypothyroid animals, the glands were studied after being stained with H and E. In the control animals, the serous acini were spherical in shape, closely packed and the acini were composed of a single layer of pyramidal cells with basophilic cytoplasm. The acini had a broad base and a narrow apex with basal, spherical nucleus and were separated by inter-acinar connective tissue (Fig. 2C). Among the acini, the intercalated ducts were lined with a single layer of cuboidal epithelial cells with central large, rounded nuclei and eosinophilic cytoplasm (Fig. 3A). The striated ducts revealed epithelial lining formed of columnar cells containing rounded nuclei in the center and possessed pale eosinophilic cytoplasm (Fig. 3D). The excretory interlobular ducts were encircled by fibrous connective tissue and were lined by columnar epithelium and had wide lumen. Additionally, blood vessels were visible in the connective tissue septa (Fig. 4A).

In the hypothyroid group, serous acini revealed an apparent smaller size with an irregular outline. The acinar cell nuclei displayed nuclear

Table 1
Comparison between the two studied groups according to Triiodothyronine and Thyroxine.

	Control rats (n = 8)	Hypothyroid rats (n = 16)	U (Mann Whitney test)	p-value
Triiodothyronine (ng/dl)				
Min. – Max.	127.0–139.5	83.70–100.4	0.00*	< 0.001*
Median (interquartile range (IQR))	130.5 (128.4–134.5)	91.92 (87.6–95.5)		
Thyroxine (μg/dl)				
Min. – Max.	8.34–9.40	5.22–6.70	0.00	< 0.001*
Median (IQR)	9.02(8.8–9.3)	5.99(5.5–6.2)		

* Statistically significant at $p \leq 0.05$

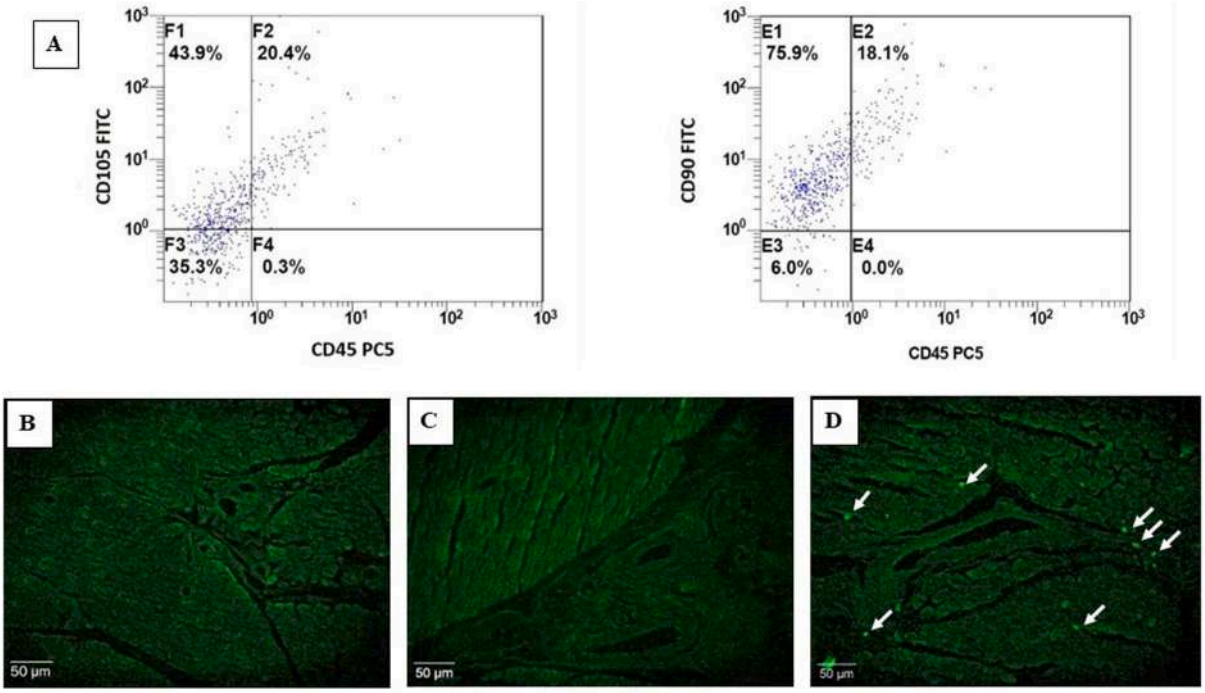

Fig. 1. Mesenchymal stem cells isolated from the bone marrow (BM-MSCs) immunophenotyping and labelling in control and hypothyroid rats. A dot blot representing flow cytometric immunophenotyping of the BM-MSCs of three-week-old rats and showing CD90, CD105 immuno-positive and CD45 immuno-negative cells, depicting pure extraction of BM-MSCs. Photomicrographs of parotid gland tissues of control male rat (B), hypothyroid rat (C) depicting negative PKH67 labelling and of BM-MSCs treated rats (D) showing green fluorescent-labelled BM-MSCs (white arrows) (PKH67, (B-D), Magnification x100).

alterations with some being pyknotic, pleomorphic or hyperchromatic. Different-sized cytoplasmic vacuoles were detected in the acinar cytoplasm (Fig. 2D). The intercalated ducts depicted indistinct borders along with abnormal nuclear configuration (Fig. 3B). The striated ducts revealed abnormal epithelium lining and nuclear morphology. The cytoplasm depicted vacuolization with apparent loss of the ductal basal striations (Fig. 3E). The epithelial lining of excretory ducts was atrophied with areas of discontinuity in the lining. The nuclei revealed abnormal configuration, and the cytoplasm depicted vacuolization. Moreover, the interlobular connective tissue showed an apparent increase in collagen fibers with dilated and congested blood vessels. Inflammatory cell infiltration was also detected (Fig. 4B).

In the HT-MSCs group, and in comparison to the HT group, most of the serous acini restored their normal architecture formed of pyramidal cells with well-defined borders, basal nuclei, and basophilic cytoplasm (Fig. 2E). The intercalated ducts depicted normal histological structure with cuboidal cell lining, and large, rounded nuclei in the center (Fig. 3C). The striated ducts revealed normal histology and were lined by columnar cells with evident basal striations (Fig. 3F). The interlobular excretory ducts revealed a continuous epithelial lining formed of columnar cells with euchromatic nuclei. The interlobular ducts were encircled by an apparent thin connective tissue layer (Fig. 4C).

3.4. Aberrant decrease in the area and perimeter of the acini of the hypothyroid rats and their restoration in the stem-cell-treated hypothyroid animals

In comparison to the controls, the acini of the HT group depicted a decrease in the acinar perimeter (670.9 ± 53.70, $p < 0.001$) and area (97.48 ± 4.15, $p < 0.001$) indicating atrophy. In the HT-MSCs group, the acinar size was restored in perimeter (1478.5 ± 29.19, $p = 0.008$), and area (148.5 ± 2.59, $p = 0.002$) compared to the HT group.

The perimeter and area of the serous acini of the HT-MSC group were insignificantly different from that of their controls (1512.9 ± 26.73, $p = 0.138$) and (149.2 ± 1.63, $p = 0.480$), respectively (Figs. 4D, 4E), (Table 2).

4. Discussion

In the present work, we evaluated the impact of the BM-MSC infusion in ameliorating the structural alterations of the parotid gland in hypothyroid male rats, utilizing experimental animal model. Hypothyroidism is a common thyroid disorder, which is characterized by decreased production of thyroid hormones (Cakic-Milosevic et al., 2004; Cano-Europa et al., 2011), and imbalance in thyroid hormones leads to pathological alterations in the salivary glands (Hayat et al., 2010, 2016; Nasr El-Din & Abdel Fattah, 2020). In our experimental model, carbimazole was utilized to induce hypothyroidism. To confirm the induction of hypothyroidism in rats treated with carbimazole, the serum level of the thyroid hormones was assessed. Our results revealed low serum levels of thyroid hormones in the animals treated with carbimazole or its active form, methimazole. Our findings are in agreement with the results of the earlier work of (Elazeem et al., 2016; Hayat et al., 2016; Arafa et al., 2018; Nasr El-Din & Abdel Fattah, 2020; El dahrawy et al., 2021; Mahmoud et al., 2024). It has been reported that the drug blocks the tyrosine residue iodination by acting as a false substrate to the thyroid peroxidase leading to low levels of thyroxine and triiodothyronine (Cakic-Milosevic et al., 2004; Sakr et al., 2016).

The parotid gland was chosen as more than half of the total volume of salivary secretion is produced by the parotid gland, making it the most significant in terms of salivary production during stimulated salivary flow (Estafanos, 2020). The systemic way of administration of BM-MSCs was utilized since it is the least invasive method, easy-to-repeat infusions, and the cells remain close to the nutrient and oxygen-rich vasculature once they have extravasated into the target tissue (Yan et al., 2021; Upadhyay & Tran, 2023).

In the current work, the parotid gland of rats with induced hypothyroidism revealed deterioration of gland architecture. The serous acini were atrophied, with an indistinct outline. In addition, the duct system showed abnormal histology. Our data confirms the findings of the

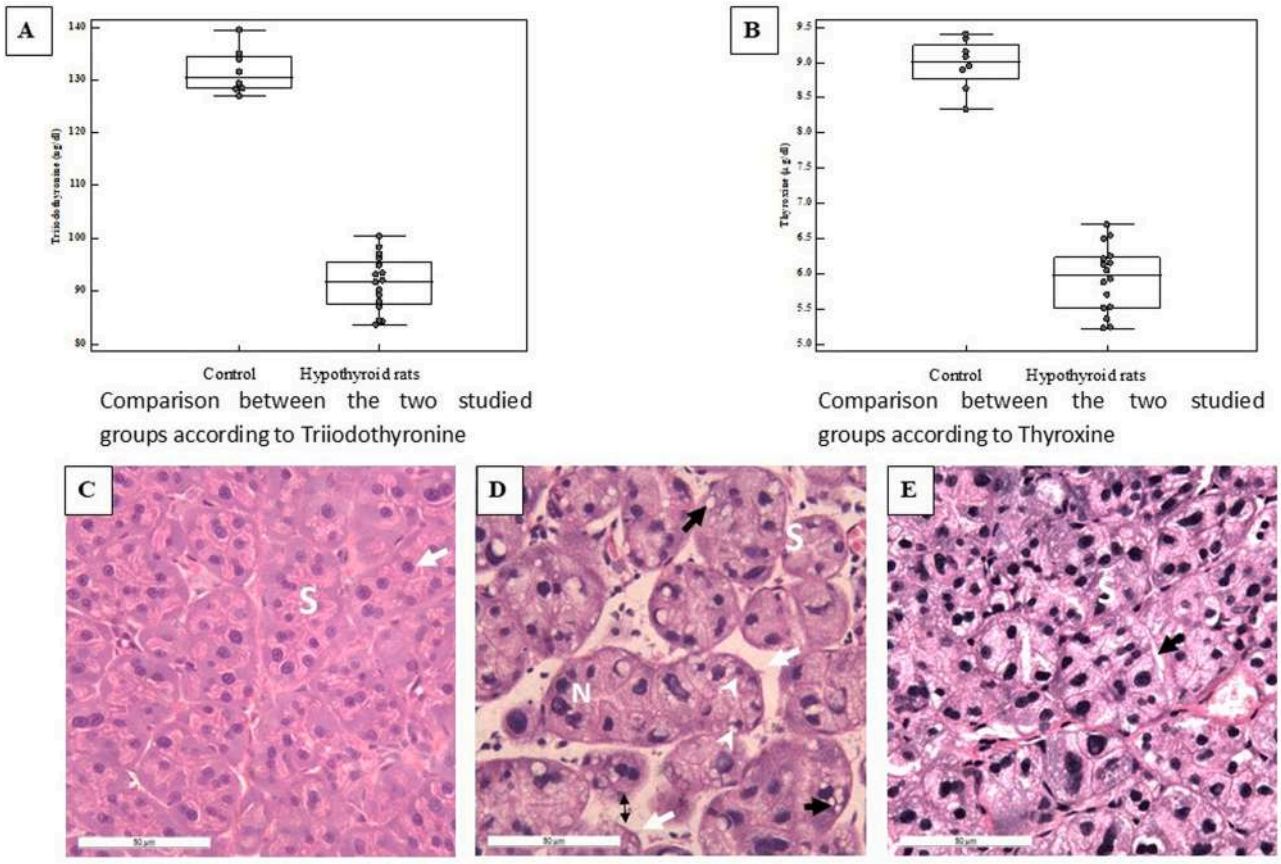

Fig. 2. Transplanted mesenchymal stem cells isolated from the bone marrow (BM-MSCs) restored the normal histology of the parotid gland acini of the hypothyroid rats. (A, B) Graph showing a comparison between the control, hypothyroid rats according to serum values of the Triiodothyronine (A) and Thyroxine (B). The hypothyroid animals depicted significantly lower serum levels of triiodothyronine $p < 0.001$, and decreased thyroxine serum level $p < 0.001$ compared to their controls. Photomicrographs of the parotid salivary gland of control rat (C) showing normal parotid tissue with normal serous acini (S) exhibiting basal rounded nuclei (white arrow); hypothyroid rat group (D) showing distorted architecture of the acini, some serous acini appear atrophied (S) with indistinct outlines (double arrow), apparently wide inter-acinar spaces (white arrows), some acinar nuclei are pyknotic (white arrowheads) or hyperchromatic (N) and cytoplasmic vacuolization of the acinar cells (black arrows) and hypothyroid rat group receiving BM-MSC injection (E) showing that most of acini restored their normal histology (S) with apparent decrease in the inter-acinar spaces (black arrows). H and E, magnification x400 (C, D, E).

previous studies on parotid gland of hypothyroid rats (Hayat et al., 2010; Ayuob, 2016; Elazeem et al., 2016; Nasr El-Din & Abdel Fattah, 2020; Uzun et al., 2022). These deleterious alterations could be due to the critical function of thyroid hormones regulating oxidative metabolism and producing free radicals (Macvanin et al., 2023). In hypothyroidism, functional changes in thyroid gland impact the body's capacity to generate reactive oxygen species and escalate oxidative stress (Chakrabarti et al., 2016; Algaidi et al., 2022), and they initiate a chain reaction that damages the cell membrane lipids and other components of the cell through oxidative damage (Chakrabarti et al., 2016; Pizzino et al., 2017). Furthermore, individuals with hypothyroidism have impaired antioxidant defence mechanisms across various structures (Kandasamy et al., 2021).

In this work, the nuclei of the parotid acini and of the duct system depicted abnormal morphology including nuclear pyknosis and hyperchromatism. Similar results were demonstrated in previous studies (Hayat et al., 2010; Ayuob, 2016; Elazeem et al., 2016; Uzun et al., 2022). It has been reported that cellular metabolic activity is associated with large euchromatic nuclei (Björk & Wieslander, 2014) and high percentage of heterochromatin is indicative of low metabolic activity of the cells (Ashour, 1998). Taken together, these data suggest low metabolic activity and impaired function in the parotid gland of hypothyroid rats.

Furthermore, in the current work, the hypothyroid rats displayed vacuolization in the acinar and ductal cytoplasm. This is consistent with earlier research on parotid glands of hypothyroid animals (Hayat et al., 2010; Elazeem et al., 2016; Nasr El-Din & Abdel Fattah, 2020). These vacuoles may be autophagic or lipid-filled vacuoles. Lipid accumulation has been linked to a decrease in the synthesis of secretory granules (Yashida et al., 2011). It has been reported that extreme vacuolization may cause apoptosis or cell death (Henics & Wheatley, 1999).

In the present work, parotid acini of the hypothyroid group were atrophied and had decreased size and perimeter compared to the controls. Similar to our findings, atrophic alterations in the serous acini of parotid gland of rats with induced hypothyroidism were reported (Hayat et al., 2010; Ayuob, 2016; Elazeem et al., 2016; Uzun et al., 2022). It has been suggested that acinar atrophy in the parotid gland and also in the submandibular gland of methimazole-induced hypothyroidism in rats may be due to diminished function of the parotid gland (Hayat et al., 2010) and submandibular gland (Hayat et al., 2016).

In this study, the parotid gland of rats with hypothyroidism depicted an apparent increase in the collagen fiber layer encircling the interlobular ducts, with inflammatory cellular infiltrate. Our findings are in agreement with the earlier results of Elazeem et al., (2016). It has been reported that in the injured tissues, the extracellular matrix is reconstructed and the inflammatory factors are released followed by the formation of extracellular matrix components including collagen (Kramann et al., 2013; Qin et al., 2023). It has been reported that transplanted MSCs have protective effect against fibrotic disorders by their ability to modify the fibrotic environment and the injured cells by

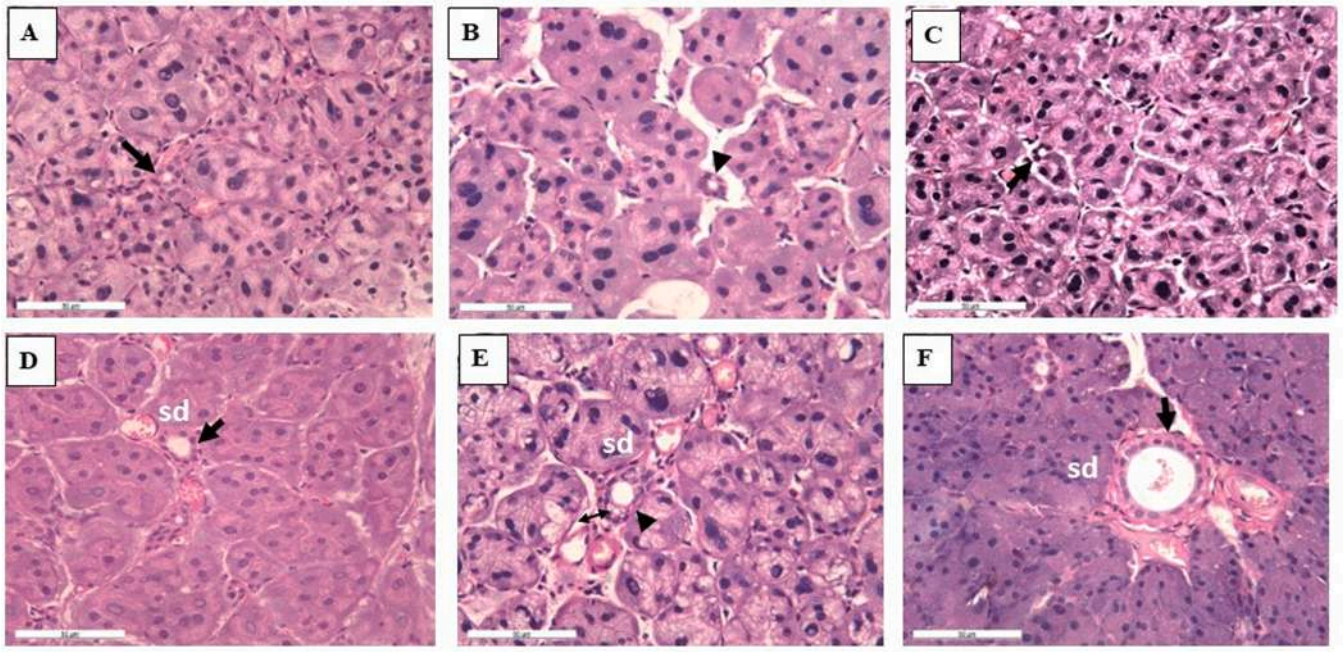

Fig. 3. Infused mesenchymal stem cells isolated from the bone marrow (BM-MSCs) recovered the altered histology in intercalated and striated ducts in the hypothyroid rats. Photomicrographs of intercalated ducts of the parotid salivary gland of control group (A) depicting normal histology with cuboidal cells with central rounded nuclei and eosinophilic cytoplasm (black arrows); hypothyroid rat group (HT group)(B) showing intercalated duct with ill-defined borders and abnormal configurations (black arrowhead) and the hypothyroid rat group receiving BM-MSC injection (HT-MSC group) (C) showing restoration of the normal cellular architecture of the ductal epithelium (black arrow). Representative images of the striated duct (Sd) depicting central nuclei in the control group (D) (black arrows); Sd of the HT group (E) depicting abnormal nuclear morphology, loss of basal striations (black arrowhead) and vacuolization of the cytoplasm (double arrow) and Sd of the HT-MSC group (F) showing restoration of the normal cellular configuration of the ductal epithelium with restoration of the basal striations (black arrows). H and E, magnification x400 (A-F).

both indirect and direct effect (Qin et al., 2023).

There is no effective pharmacological therapy or palliative care for hyposalivation induced by structural salivary gland alterations. Saliva substitutes and oral lubricants have inconsistent ability to relieve symptoms of hyposalivation and are short lived. In addition, saliva stimulants´effect is depending on the residual gland function and is of limited effect in cases of severe glandular hypofunction (Chibly et al., 2022). Cell based therapy which utilized isolated living cells to resume the gland structure and function have developed large step forward in treating salivary gland dysfunction (Chibly et al., 2022). The BM-MSCs are the most commonly used MSCs, easy to extract and culture and feasible for allogenic and autologous cell-based therapy (Musiał-Wysocka et al., 2019). In the present work, hypothyroid animals infused with the BM-MSCs displayed restoration of the normal architecture of the acini and ducts with distinct borders, normal nuclear histology and near absence of the acinar and ductal vacuolization. Various *in vivo* studies reported the regenerative capacity of MSCs derived from the bone marrow in several organs, including the parotid gland. Transplanted BM-MSCs regenerate the structural alterations in pancreas of hypothyroid rats (Arafa et al., 2018); in the injured tissues of the parotid salivary glands in rats with ovariectomy (Abd El-Haleem et al., 2018) and also in rats with streptozotocin-induced diabetes (Denewar & Amin, 2020), in parotid gland changes of cisplatin-treated rats (Abdelaziz et al., 2023), the cytotoxic alterations induced by cisplatin in the submandibular gland (Zakaria et al., 2025), histopathological changes of the submandibular gland of ovariectomized rats (El-Badawy et al., 2024) and in the structural alterations of the tongue of rats with induced hypothyroidism (Mahmoud et al., 2024). This reparative effect of the transplanted stem cells could be attributed to the large amounts of cytokines, growth factors, and chemokines released from these cells, including transforming growth factor-beta, interleukin 6, 10, and vascular endothelial growth factor which facilitates their migration and proliferation, immunosuppressive effects, and regulation of angiogenesis and apoptosis (Augello et al., 2010; Gebler et al., 2012; Han et al., 2022). Furthermore, MSCs can integrate into tissues and characterize to various identities of cells (Afshari et al., 2020).

Canonical Wnt transduction cascade is crucial in tissue regeneration and adult stem cell maintenance. Different components of the cascade are detected in the adult salivary glands of human and mice (Hoffman et al., 2002; Sun et al., 2008). In adult mouse, canonical Wnt signaling is active in the duct system and is increased during the regeneration of the injured salivary gland. In addition, hedgehog signaling was also increased (Hai et al., 2010). It has been reported that activation of canonical Wnt transduction cascade can alleviate hyposalivation by maintaining the stem/progenitor cells and inhibiting apoptosis (Goessling et al., 2008). Various signaling pathways are involved in the salivary gland development including retinoic acid (Lohnes et al., 1994), FGF signaling (Steinberg et al., 2005), and notch signaling (García-Gallastegui et al., 2014). Future research is needed to discern whether the role of BM-MSCs in alleviating parotid gland abnormalities in hypothyroid rats is operated by any of the above mentioned signaling cascades.

The limitation of this study was the lack of evaluation of the functional changes and of the molecular alterations in the parotid gland of hypothyroid rats that require further studies. Future studies are in need to evaluate the possible ameliorative impact of BM-MSC therapy on the altered histology of parotid glands in hypothyroid patients who suffer from impaired salivary function consequences.

5. Conclusion

Hypothyroidism induction in male rats resulted in histological alterations in the parotid gland. The glandular tissues depicted apparently acinar atrophy with decreased area and perimeter, nuclear changes and cytoplasmic vacuolization. The duct system depicted distorted epithelial wall lining of the excretory, striated and intercalated ducts. BM-MSC

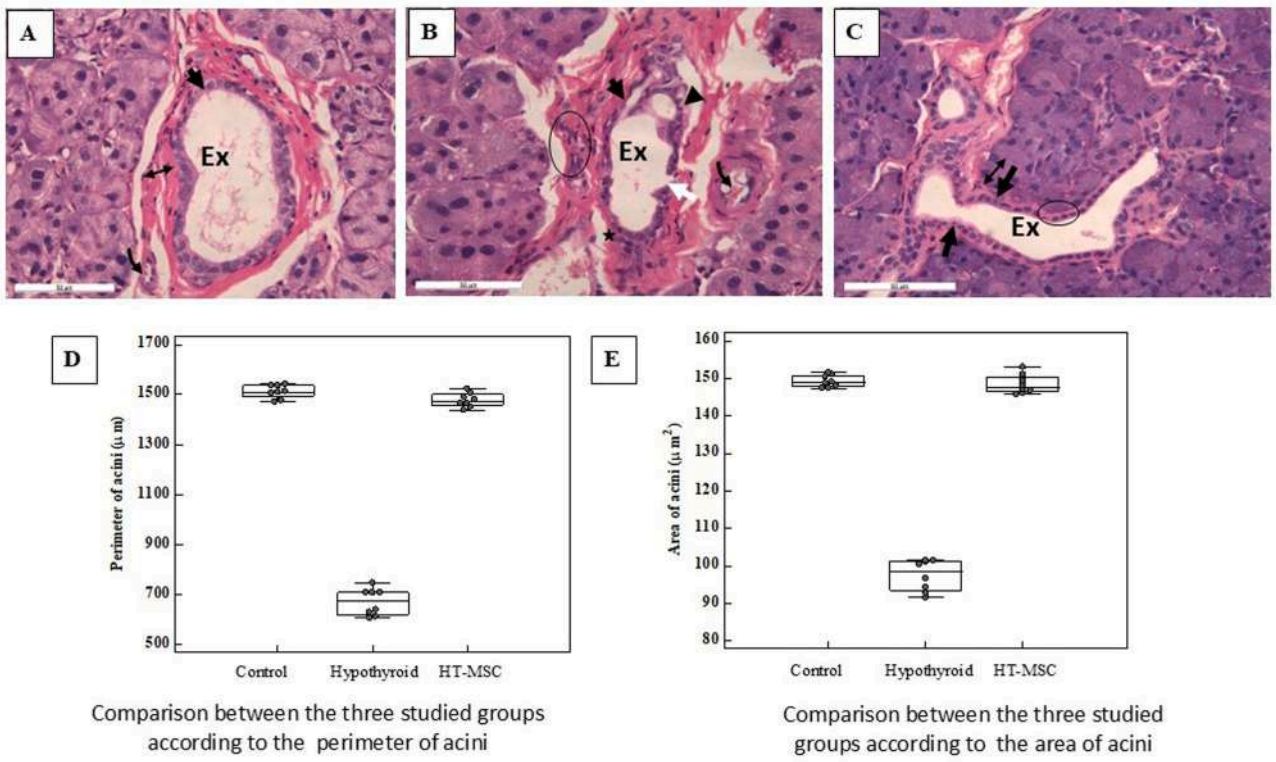

Fig. 4. Administration of the mesenchymal stem cells isolated from the bone marrow (BM-MSCs) rescued the abnormal histology of the excretory ducts in the hypothyroid rats. Photomicrographs of the interlobular excretory ducts (Ex) of the parotid salivary gland of control group (A) showing wide lumen and lined with columnar epithelium (black arrow) and surrounded by connective tissue fibers (double arrow), with patent blood vessels (black curved arrow); Ex of the hypothyroid rat group (HT group)(B) depicting loss of cellular arrangement with atrophied epithelium (black arrow), discontinuity at some areas (white arrow), the nuclei show hyperchromatic (asterisk) and pyknotic (black arrowhead) appearance and the duct is surrounded by an apparently thick connective tissue layer with dilated blood vessel (black curved arrow) and inflammatory cellular infiltrate (circle) seen within it; and Ex of the hypothyroid rat group receiving BM-MSC injection (HT-MSC group)(C) showing near restoration of the normal histology (black arrows), nuclear morphology (circle), and with apparently thin surrounding fibrous tissue (double arrow). (H and E, magnification x400 (A, B &C)). (D, E) Graphs showing comparison between the control, HT and HT-MSC groups according to the perimeter (D) and area (E) of acini. The hypothyroid rats showed significantly decreased acinar perimeter $p < 0.001$ and area $p < 0.001$ compared to the control animals. The HT-MSC group showed restoration of the acinar perimeter $p = 0.008$ and area $p = 0.002$ compared to the HT group. The HT-MSC group depicted insignificant differences in area $p = 0.480$ and perimeter $p = 0.138$, in comparison to the controls.

Table 2
Comparison between the three studied groups according to acini perimeter and area.

	Control (n = 8)	Hypothyroid (n = 8)	HT-MSC (n = 8)	H (Kruskal Wallis test)	P-value
Perimeter of acini (μm)					
Min. – Max.	1472.2 – 1543.9	607.2 – 747.1	1437.7 – 1525.3	17.565*	< 0.001*
Median (interquartile range (IQR))	1512.1[a](1494.0 – 1537.4)	675.3[b](621.7 – 709.6)	1473.7[a](1458.6 – 1500.3)		
Sig. bet. grps.	$p_1 < 0.001$*, $p_2 = 0.138$, $p3 = 0.008$*				
Area of acini (μm²)					
Min. – Max.	147.4 – 151.6	91.62 – 101.5	145.8 – 153.2	15.860*	< 0.001*
Median (IQR)	148.9[a]) 147.8 – 150.8)	98.55[b](93.6 – 101.3)	147.7[a](146.4 – 150.2)		
Sig. bet. grps.	$p_1 < 0.001$*, $p_2 = 0.480$, $p3 = 0.002$*				

The p-value for comparison between the groups was as follows; p_1 for comparing between **Control** and **Hypothyroid groups**, p_2 for comparing between **Control** and **HT-MSCs groups** and p_3 comparing between **Hypothyroid** and **HT-MSCs groups.** Medians with **Small Common letters (a-b)** are not significant (**OR** Medians with **different letters (a-b)** are significant).

* Statistically significant at $p \leq 0.05$

transplantation regained the normal architecture, area and perimeter of the acini and ductal histology, thus ameliorating the degenerative effect of hypothyroidism on the parotid gland, suggesting restored function of the parotid tissues.

Funding

This research did not receive any specific grant from funding agencies in the public, commercial or not-for-profit sectors.

CRediT authorship contribution statement

Maha El Shahawy: Writing – review & editing, Writing – original draft, Visualization, Validation, Supervision, Resources, Project administration, Methodology, Investigation, Formal analysis, Data curation, Conceptualization. **Mohamed Badawy:** Writing – review & editing, Visualization, Validation, Supervision. **Mary Moheb:** Writing – review & editing, Visualization, Validation, Supervision. **Hanan El-Hemedy:** Writing – review & editing, Writing – original draft, Visualization, Validation, Resources, Methodology, Investigation, Funding acquisition,

Formal analysis, Data curation.

Declaration of Competing Interest

We wish to confirm that there are no known conflicts of interest associated with this publication and there has been no significant financial support for this work that could have influenced its outcome.

Acknowledgements

None

Data availability

All data are available from the corresponding author upon a reasonable request

References

Abd El-Haleem, M. R., Selim, A. O., & Attia, G. M. (2018). Bone marrow–derived mesenchymal stem cells ameliorate parotid injury in ovariectomized rats. *Cytotherapy, 20*(2), 204–217. https://doi.org/10.1016/j.jcyt.2017.10.003

Abdel Fattah, H. S., & Omar, E. M. (2023). The protective role of curcumin nanoparticles on the submandibular salivary gland toxicity induced by methotrexate in Male rats. *Archives of Oral Biology, 152*, Article 105717. https://doi.org/10.1016/j.archoralbio.2023.105717

Abdelaziz, A., sherif, H., & mawla, A.E. A.El (2023). *Effect of bone marrow mesenchymal stem cells on cisplatin induced cytotoxicity in parotid gland of rats (Histological and Ultrastructural studies)*. https://doi.org/10.21203/rs.3.rs-3663849/v1.

Abdelwahed, M. H. A. E., Badreldin, M. H., Ibrahim, I. H., Zittoon, R. F., Galhom, R. A., Mohammed, S. S., & Ashry, Y. M. (2025). The potential of bone marrow derived mesenchymal stem cells in treating cisplatin induced sensorineural hearing loss in a Guinea pig animal model. *Tissue and Cell, 93*, Article 102703. https://doi.org/10.1016/j.tice.2024.102703

Afshari, A., Shamdani, S., Uzan, G., Naserian, S., & Azarpira, N. (2020). Different approaches for transformation of mesenchymal stem cells into hepatocyte-like cells. *Stem Cell Research Therapy, 11*(1), 54. https://doi.org/10.1186/s13287-020-1555-8

Ajayi, A.F., Adelakun, A., & Akhigbe, R.E. (2018). *Gastric Mucosa Damage and Impairment of Secondary Immune Response in Dysthyroidism is Associated with TNF-α Expression*. ⟨https://www.researchgate.net/publication/322357901⟩.

Algaidi, S. A., Faddladdeen, K. A., Alrefaei, G. I., Qahl, S. H., Albadawi, E. A., ALmohaimeed, H. M., & Ayuob, N. N. (2022). Thymoquinone protects the testes of hypothyroid rats by suppressing pro-inflammatory cytokines and oxidative stress and promoting SIRT1 testicular expression. *Frontiers in Pharmacology, 13*. https://doi.org/10.3389/fphar.2022.1040857

Alhahawachee, Z., Al Allaf, luma, & Taqa, G. (2022). Effect of hypothyroidism on submandibular salivary gland histology in rat: role of ashwagandha root extract versus thyroid hormone, 0–0 *Egyptian Journal of Histology, 0*(0). https://doi.org/10.21608/ejh.2022.139804.1689.

Al-Serwi, R. H., El-Kersh, A. O. F. O., & El-Akabawy, G. (2021). Human dental pulp stem cells attenuate streptozotocin-induced parotid gland injury in rats. *Stem Cell Research Therapy, 12*(1), 577. https://doi.org/10.1186/s13287-021-02646-6

Al-Suhaimi, E. A., & Khan, F. A. (2022). Thyroid glands: physiology and structure. *Emerging Concepts in Endocrine Structure and Functions* (pp. 133–160). Springer Nature Singapore. https://doi.org/10.1007/978-981-16-9016-7_5

Arafa, M. A. A., Gouda, Z. A., El-naseery, N. I., Abdel-Nour, H. M., Hanafy, S. M., Mohamed, A. F., & Abo-Ouf, A. M. (2018). Bone Marrow-Derived mesenchymal stem cells ameliorate the pancreatic changes of chemically induced hypothyroidism by carbimazole in Male rats. *Cells Tissues Organs, 206*(3), 144–156. https://doi.org/10.1159/000497297

Ashour. (1998). Long- term effect of melatonin on submandibular salivary glands in old rats. *EMHJ - Eastern Mediterranean Health Journal, 4*(2), 324–331. ⟨https://iris.who.int/handle/10665/118173⟩.

Augello, A., Kurth, T., & De Bari, C. (2010). Mesenchymal stem cells: a perspective from in vitro cultures to in vivo migration and niches. *European Cells and Materials, 20*, 121–133. https://doi.org/10.22203/eCM.v020a11

Ayuob, N. N. (2016). Histological and immunohistochemical study on the possible ameliorating effects of thymoquinone on the salivary glands of rats with experimentally induced hypothyroidism. *The Egyptian Journal of Histology, 39*(2), 125–135. https://doi.org/10.1097/01.EHX.0000489145.55478.51

Björk, P., & Wieslander, L. (2014). Mechanisms of mRNA export. *Seminars in Cell Developmental Biology, 32*, 47–54. https://doi.org/10.1016/j.semcdb.2014.04.027

Bordbar, H., Sattar-Shamsabadi, M., Dehghani, F., & Karimi, F. (2024). Protective effect of platelet-rich plasma against structural and functional changes of the adult rat testis in carbimazole-induced hypothyroidism. *Clinical and Experimental Reproductive Medicine*. https://doi.org/10.5653/cerm.2023.06695

Cakic-Milosevic, M., Korac, A., & Davidovic, V. (2004). Methimazole-induced hypothyroidism in rats: effects on body weight and histological characteristics of thyroid gland. *Jugoslovenska Medicinska Biohemija, 23*(2), 143–147. https://doi.org/10.2298/JMH0402143C

Cano-Europa, E., Blas-Valdivia, V., Franco-Colin, M., Gallardo-Casas, C. A., & Ortiz-Butrón, R. (2011). Methimazole-induced hypothyroidism causes cellular damage in the spleen, heart, liver, lung and kidney. *Acta Histochemica, 113*(1), 1–5. https://doi.org/10.1016/j.acthis.2009.07.004

Cardiff, R. D., Miller, C. H., & Munn, R. J. (2014). Manual hematoxylin and eosin staining of mouse tissue sections. *Cold Spring Harbor Protocols, 2014*(6), Article pdb.prot073411. https://doi.org/10.1101/pdb.prot073411

Chakrabarti, S., Ghosh, S., Banerjee, S., Mukherjee, S., & Chowdhury, S. (2016). Oxidative stress in hypothyroid patients and the role of antioxidant supplementation. *Indian Journal of Endocrinology and Metabolism, 20*(5), 674. https://doi.org/10.4103/2230-8210.190555

Chibly, A. M., Aure, M. H., Patel, V. N., & Hoffman, M. P. (2022). Salivary gland function, development, and regeneration. *Physiological Reviews, 102*(3), 1495–1552. https://doi.org/10.1152/physrev.00015.2021

Council. (2011). *Guide for the care and use of laboratory animals*. National Academies Press. https://doi.org/10.17226/12910

Denewar, M., & Amin, L. E. (2020). Role of bone marrow-derived mesenchymal stem cells on the parotid glands of streptozotocin induced diabetes rats. *Journal of Oral Biology and Craniofacial Research, 10*(2), 33–37. https://doi.org/10.1016/j.jobcr.2020.02.003

El dahrawy, dina, Adawy, H., & eldeeb, mona (2021). Effect of bone marrow Derived-Mesenchymal stem cells on submandibular salivary glands of carbimazole induced hypothyroidism in albino rats, 0–0 *Al-Azhar Dental Journal for Girls, 0*(0). https://doi.org/10.21608/adjg.2021.29129.1252.

Elazeem, A. A., Mohammed, M. Z., & Hassan, E. Z. (2016). Effect of experimentally induced hypothyroidism on the parotid gland of adult Male albino rats and the possible role of thyroid hormone supplementation. *British Journal of Science, 14*(1).

El-Badawy, M. A., Badawy, M., & El Shahawy, M. (2024). Bone marrow derived mesenchymal stem cells restored GLUT1 expression in the submandibular salivary glands of ovariectomized rats. *Archives of Oral Biology, 166*, Article 106048. https://doi.org/10.1016/j.archoralbio.2024.106048

El-naseery, N. I., Elewa, Y. H. A., Ichii, O., & Kon, Y. (2018). An experimental study of menopause induced by bilateral ovariectomy and mechanistic effects of mesenchymal stromal cell therapy on the parotid gland of a rat model. *Annals of Anatomy, 220*, 9–20. https://doi.org/10.1016/j.aanat.2018.06.006

Estafanos, R. (2020). *Extemporaneously compounded buccal pilocarpine preparations, acceptability and pilot testing for the treatment of xerostomia (dry mouth) in Australia* [The University of Queensland]. https://doi.org/10.14264/uql.2020.646.

Fathi, E., & Farahzadi, R. (2022). Mesenchymal stem cells as a Cell-Based therapeutic strategy targeting the telomerase activity of KG1 acute myeloid leukemia cells. *ACTA MEDICA IRANICA*. https://doi.org/10.18502/acta.v60i2.8817

García-Gallastegui, P., Ibarretxe, G., Garcia-Ramírez, J.-J., Baladrón, V., Aurrekoetxea, M., Nueda, M.-L., Naranjo, A.-I., Santaolalla, F., Sánchez-del Rey, A., Laborda, J., & Unda, F. (2014). DLK1 regulates branching morphogenesis and parasympathetic innervation of salivary glands through inhibition of NOTCH signalling. *Biology of the Cell, 106*(8), 237–253. https://doi.org/10.1111/boc.201300086

Gebler, A., Zabel, O., & Seliger, B. (2012). The immunomodulatory capacity of mesenchymal stem cells. *Trends in Molecular Medicine, 18*(2), 128–134. https://doi.org/10.1016/j.molmed.2011.10.004

Ghannam, M.G., & Singh, P. (2022). *Anatomy, Head and Neck, Salivary Glands*.

Goessling, W., North, T. E., Lord, A. M., Ceol, C., Lee, S., Weidinger, G., Bourque, C., Strijbosch, R., Haramis, A.-P., Puder, M., Clevers, H., Moon, R. T., & Zon, L. I. (2008). APC mutant zebrafish uncover a changing temporal requirement for wnt signaling in liver development. *Developmental Biology, 320*(1), 161–174. https://doi.org/10.1016/j.ydbio.2008.05.526

Hai, B., Yang, Z., Millar, S. E., Choi, Y. S., Taketo, M. M., Nagy, A., & Liu, F. (2010). Wnt/β-catenin signaling regulates postnatal development and regeneration of the salivary gland. *Stem Cells and Development, 19*(11), 1793–1801. https://doi.org/10.1089/scd.2009.0499

Han, Y., Yang, J., Fang, J., Zhou, Y., Candi, E., Wang, J., Hua, D., Shao, C., & Shi, Y. (2022). The secretion profile of mesenchymal stem cells and potential applications in treating human diseases. *Signal Transduction and Targeted Therapy, 7*(1), 92. https://doi.org/10.1038/s41392-022-00932-0

Hashem, H., & Saad, S. (2019). Comparative study of the effect of experimentally induced hyperthyroidism and hypothyroidism on the parotid gland in adult Male albino rats, 0–0 *Egyptian Journal of Histology, 0*(0). https://doi.org/10.21608/ejh.2019.17411.1174.

Hayat, N. Q., Nadir, S., & Farooq, M. U. (2016). Histological characteristics of submandibular gland after induction of hypothyroidism in adult albino rat. *In Journal of Rawalpindi Medical College (JRMC), 20*(1). ⟨https://www.journalrmc.com/index.php/JRMC/article/view/216/96⟩.

Hayat, N. Q., Tahir, M., Munir, B., & Sami, W. (2010). Effect of methimazole-induced hypothyroidism on histological characteristics of parotid gland of albino rat. *Journal of Ayub Medical College, Abbottabad: JAMC, 22*(3), 22–27. ⟨https://pubmed.ncbi.nlm.nih.gov/22338410/⟩.

Heidari, H. R., Fathi, E., Montazersaheb, S., Mamandi, A., Farahzadi, R., Zalavi, S., & Nozad Charoudeh, H. (2021). Mesenchymal stem cells cause telomere length reduction of Molt-4 cells via Caspase-3, BAD and P53 apoptotic pathway. *International Journal of Molecular and Cellular Medicine, 10*(2), 113–122. https://doi.org/10.22088/IJMCM.BUMS.10.2.113

Henics, T., & Wheatley, D. N. (1999). Cytoplasmic vacuolation, adaptation and cell death: a view on new perspectives and features. *Biology of the Cell, 91*(7), 485–498. https://doi.org/10.1016/S0248-4900(00)88205-2

Hoffman, M. P., Kidder, B. L., Steinberg, Z. L., Lakhani, S., Ho, S., Kleinman, H. K., & Larsen, M. (2002). Gene expression profiles of mouse submandibular gland

development: FGFR1 regulates branching morphogenesis in vitro through BMP- and FGF-dependent mechanisms. *Development, 129*(24), 5767–5778. https://doi.org/10.1242/dev.00172

Hofstee, P., Bartho, L. A., McKeating, D. R., Radenkovic, F., McEnroe, G., Fisher, J. J., Holland, O. J., Vanderlelie, J. J., Perkins, A. V., & Cuffe, J. S. M. (2019). Maternal selenium deficiency during pregnancy in mice increases thyroid hormone concentrations, alters placental function and reduces fetal growth. *The Journal of Physiology, 597*(23), 5597–5617. https://doi.org/10.1113/JP278473

Ito, K., Izumi, N., Funayama, S., Nohno, K., Katsura, K., Kaneko, N., & Inoue, M. (2023). Characteristics of medication-induced xerostomia and effect of treatment. *PloS One, 18*(1), Article e0280224. https://doi.org/10.1371/journal.pone.0280224

Jammes, M., Tabasi, A., Bach, T., & Ritter, T. (2025). Healing the cornea: exploring the therapeutic solutions offered by MSCs and MSC-derived EVs. *Progress in Retinal and Eye Research, 105*, Article 101325. https://doi.org/10.1016/j.preteyeres.2024.101325

Kandasamy, B., Jayaraaj, I. A., & Prabhakar, J. (2021). Influence of abnormal thyroid hormone changes on lipid peroxidation and antioxidant imbalance in hypothyroid and hyperthyroid patients. In *Highlights on Medicine and Medical Research, 12* pp. 159–167). Book Publisher International (a part of SCIENCEDOMAIN International). https://doi.org/10.9734/bpi/hmmr/v12/2178F

Kramann, R., DiRocco, D. P., Maarouf, O. H., & Humphreys, B. D. (2013). Matrix-Producing cells in chronic kidney disease: origin, regulation, and activation. *Current Pathobiology Reports, 1*(4), 301–311. https://doi.org/10.1007/s40139-013-0026-7

Kurup, A., Ravindranath, S., Tran, T., Keating, M., Gascard, P., Valdevit, L., Tlsty, T. D., & Botvinick, E. L. (2015). Novel insights from 3D models: the pivotal role of physical symmetry in epithelial organization. *Scientific Reports, 5*. https://doi.org/10.1038/srep15153

Lohnes, D., Mark, M., Mendelsohn, C., Dollé, P., Dierich, A., Gorry, P., Gansmuller, A., & Chambon, P. (1994). Function of the retinoic acid receptors (RARs) during development: (I) craniofacial and skeletal abnormalities in RAR double mutants. *Development, 120*(10), 2723–2748. https://doi.org/10.1242/dev.120.10.2723

Macvanin, M. T., Gluvic, Z., Zafirovic, S., Gao, X., Essack, M., & Isenovic, E. R. (2023). The protective role of nutritional antioxidants against oxidative stress in thyroid disorders. *Frontiers in Endocrinology, 13*. https://doi.org/10.3389/fendo.2022.1092837

Mahmoud, H., Badawy, M., Mohammed, S. A.-N., & El Shahawy, M. (2024). Locally injected bone marrow-derived mesenchymal stem cells reverts the histopathological changes in the tongue of carbimazole-induced hypothyroidism of Male rats. *Archives of Oral Biology, 165*, Article 106010. https://doi.org/10.1016/j.archoralbio.2024.106010

Mohsen, R. O. M., Halawa, A. M., & Hassan, R. (2019). Role of bone marrow-derived stem cells versus insulin on filiform and fungiform papillae of diabetic albino rats (light, fluorescent and scanning electron microscopic study). *Acta Histochemica, 121*(7), 812–822. https://doi.org/10.1016/j.acthis.2019.07.007

Mostafa, S. A. R. (2022). Possible protective role of L-thyroxin on the parotid gland of adult Male albino rat in carbimazole induced hypothyroidism: histological, histomorphometry and ultrastructural study. *European Journal of Anatomy, 26*(1), 57–72. https://doi.org/10.52083/BGEK9578

Muallah, D., Matschke, J., Kappler, M., Kroschwald, L. M., Lauer, G., & Eckert, A. W. (2023). Dental pulp stem cells for salivary gland Regeneration—Where are we today? *International Journal of Molecular Sciences, 24*(10), 8664. https://doi.org/10.3390/ijms24108664

Musiał-Wysocka, A., Kot, M., & Majka, M. (2019). The pros and cons of mesenchymal stem Cell-Based therapies. *Cell Transplantation, 28*(7), 801–812. https://doi.org/10.1177/0963689719837897

Nam, K., dos Santos, H. T., Maslow, F., Small, T., Samuel, R. Z., Lei, P., Andreadis, S. T., & Baker, O. J. (2023). Fibrin hydrogels fortified with FGF-7/10 and laminin-1 peptides promote regeneration of irradiated salivary glands. *Acta Biomaterialia, 172*, 147–158. https://doi.org/10.1016/j.actbio.2023.10.013

Nanci, A. (2018). *Salivary Glands. In Ten Cate's Oral Histology; Development, Structure, and Function (9th ed.)*.

Nasr El-Din, W. A., & Abdel Fattah, I. O. (2020). Histopathological and biochemical alterations of the parotid gland induced by experimental hypothyroidism in adult Male rats and the possible therapeutic effect of nigella sativa oil. *Tissue and Cell, 65*. https://doi.org/10.1016/j.tice.2020.101366

Percie du Sert, N., Hurst, V., Ahluwalia, A., Alam, S., Avey, M. T., Baker, M., Browne, W. J., Clark, A., Cuthill, I. C., Dirnagl, U., Emerson, M., Garner, P., Holgate, S. T., Howells, D. W., Karp, N. A., Lazic, S. E., Lidster, K., MacCallum, C. J., Macleod, M., … Würbel, H. (2020). The ARRIVE guidelines 2.0: updated guidelines for reporting animal research. *Experimental Physiology, 105*(9), 1459–1466. https://doi.org/10.1113/EP088870

Pimentel, A. C. L., Rodriguez, T. T., Martins, M. D., Filho, L. C. R., Mota, I. F. S., de Carvalho Monteiro, J. S., Manieri, P. R., Pinheiro, A. L. B., Cury, P. R., & Dos Santos, J. N. (2022). Impact of photobiomodulation therapy on the morphological aspects of submandibular gland submitted to excretory duct ligation and hypothyroidism: an animal study. *Lasers in Medical Science, 37*(3), 2005–2015. https://doi.org/10.1007/s10103-021-03463-2

Pizzino, G., Irrera, N., Cucinotta, M., Pallio, G., Mannino, F., Arcoraci, V., Squadrito, F., Altavilla, D., & Bitto, A. (2017). Oxidative stress: harms and benefits for human health. *Oxidative Medicine and Cellular Longevity, 2017*, 1–13. https://doi.org/10.1155/2017/8416763

Qin, L., Liu, N., Bao, C., Yang, D., Ma, G., Yi, W., Xiao, G., & Cao, H. (2023). Mesenchymal stem cells in fibrotic diseases—the two sides of the same coin. *Acta Pharmacologica Sinica, 44*(2), 268–287. https://doi.org/10.1038/s41401-022-00952-0

Quimby, A. E., Hogan, D., Khalil, D., Hearn, M., Nault, C., & Johnson-Obaseki, S. (2020). Coconut oil as a novel approach to managing Radiation-Induced xerostomia: a primary feasibility study. *International Journal of Otolaryngology, 2020*, 1–6. https://doi.org/10.1155/2020/8537643

Radwan, I. A., Rady, D., Ramadan, M., & El Moshy, S. (2024). Mechanism underlying the anti-diabetic potential of bee venom as compared to bone marrow mesenchymal stem cells in the diabetic rat tongue. *Dental and Medical Problems, 61*(1), 53–64. https://doi.org/10.17219/dmp/152924

Ramadan Samaha, S. (2016). ACUTE EXERCISE TOLERANCE IN EXPERIMENTALLY-INDUCED HYPERTHYROIDISM IN ADULT Male ALBINO RATS. *Al-Azhar Medical Journal, 45*(2), 277–286. https://doi.org/10.12816/0029127

Reyad, A., Adawy, H., & Abdel Moneim, R. (2021). The potential therapeutic effect of allogenic bone marrow derived mesenchymal stem cells on Carbimazole-Induced hypothyroidism on albino Rats' tongue. *Al-Azhar Dental Journal for Girls, 8*(3), 451–459. https://doi.org/10.21608/adjg.2021.29218.1256

Sakr, S. A., El Nabi, S. E. H., Okdah, Y. A., El-Garawani, I. M., & Els-Shabka, A. M. (2016). Cytoprotective effects of aqueous ginger (Zingiber officinale) extract against carbimazole-induced toxicity in albino rats. *E J P Megye R, 3*(7), 489–497. ⟨https://api.semanticscholar.org/CorpusID:250501130⟩.

Schneider, S. A., Tschaidse, L., & Reisch, N. (2023). Thyroid disorders and movement Disorders—A systematic review. *Movement Disorders Clinical Practice, 10*(3), 360–368. https://doi.org/10.1002/mdc3.13656

Steinberg, Z., Myers, C., Heim, V. M., Lathrop, C. A., Rebustini, I. T., Stewart, J. S., Larsen, M., & Hoffman, M. P. (2005). FGFR2b signaling regulates ex vivo submandibular gland epithelial cell proliferation and branching morphogenesis. *Development, 132*(6), 1223–1234. https://doi.org/10.1242/dev.01690

Sun, Q., Sun, Q., Du, J., & Wang, S. (2008). Differential gene expression profiles of normal human parotid and submandibular glands. *Oral Diseases, 14*(6), 500–509. https://doi.org/10.1111/j.1601-0825.2007.01408.x

Upadhyay, A., & Tran, S. D. (2023). Stem cell therapy for salivary gland regeneration after radiation injury. *Expert Opinion on Biological Therapy, 23*(6), 455–460. https://doi.org/10.1080/14712598.2023.2199123

Uzun, S., Tatlıpınar, A., Kınal, E., Keskin, S., Özbeyli, D., & Güneş, P. (2022). Histopathological changes of parotid and larynx in hypothyroid rats: experimental study. *European Archives of Oto-Rhino-Laryngology, 279*(3), 1509–1517. https://doi.org/10.1007/s00405-021-06921-3

Wang, Z., Ju, Z., He, L., Li, Z., Liu, Y., & Liu, B. (2017). Intraglandular transplantation of Adipose-Derived stem cells for the alleviation of Irradiation-Induced parotid gland damage in miniature pigs. *Journal of Oral and Maxillofacial Surgery, 75*(8), 1784–1790. https://doi.org/10.1016/j.joms.2016.08.001

Yan, J., Liang, J., Cao, Y., El Akkawi, M. M., Liao, X., Chen, X., Li, C., Li, K., Xie, G., & Liu, H. (2021). Efficacy of topical and systemic transplantation of mesenchymal stem cells in a rat model of diabetic ischemic wounds. *Stem Cell Research Therapy, 12*(1), 220. https://doi.org/10.1186/s13287-021-02288-8

Yang, G., Fan, X., Liu, Y., Jie, P., Mazhar, M., Liu, Y., Dechsupa, N., & Wang, L. (2023). Immunomodulatory mechanisms and therapeutic potential of mesenchymal stem cells. *Stem Cell Reviews and Reports, 19*(5), 1214–1231. https://doi.org/10.1007/s12015-023-10539-9

Yashida, M. H., Da Silva Faria, A. L. D., & José Caldeira, E. (2011). Estrogen and insulin replacement therapy modulates the expression of Insulin-Like growth Factor-I receptors in the salivary glands of diabetic mice. *The Anatomical Record, 294*(11), 1930–1938. https://doi.org/10.1002/ar.21481

Zakaria, A., Sultan, N., Nabil, N., & Elgamily, M. (2025). Exosomes derived from bone marrow mesenchymal stem cells ameliorate chemotherapeutically induced damage in rats' parotid salivary gland. *Oral and Maxillofacial Surgery, 29*(1), 39. https://doi.org/10.1007/s10006-025-01331-9

Zayed, H. M., Kheir El Din, N. H., Abu-Seida, A. M., Abo Zeid, A. A., & Ezzatt, O. M. (2024). Gingival-derived mesenchymal stem cell therapy regenerated the radiated salivary glands: functional and histological evidence in murine model. *Stem Cell Research Therapy, 15*(1), 46. https://doi.org/10.1186/s13287-024-03659-7